Electrical Power and Energy Systems 142 (2022) 108228

Contents lists available at ScienceDirect

International Journal of Electrical Power and Energy Systems

journal homepage: www.elsevier.com/locate/ijepes

Multi-terminal phase-changing soft open point SDP modeling for imbalance mitigation in active distribution networks☆

Chengwei Lou [a], Jin Yang [a,*], Eduardo Vega-Fuentes [b], Nand K. Meena [c], Liang Min [a]

[a] James Watt School of Engineering, University of Glasgow, University Avenue, Glasgow, G12 8QQ, United Kingdom
[b] Institute for Applied Microelectronics, Department of Electrical Engineering, University of Las Palmas de G. C., Las Palmas de Gran Canaria, Spain
[c] Power and Renewable Energy Industry, Enzen Global Solutions UK, Birmingham, United Kingdom

ARTICLE INFO

Keywords:
Active distribution networks
Distributed energy resources
Semidefinite programming
Soft open points
Unbalanced conditions

ABSTRACT

Active distribution networks (ADNs) are capable of mitigating phase imbalance caused by various operational conditions, including uneven growth of single-phase and intermittent distributed energy resources (DERs), incurring financial losses or costly infrastructure reinforcements. In this paper, the research gap for a flexible phase imbalance mitigating solution is addressed by proposing a multi-terminal phase-changing soft open point (PC-SOP). It is explored in detail on balancing the power flows and compared with other different types and ways of connection (including two-terminal and conventional). Then operational strategies based on different cases are presented for imbalance mitigation. Semidefinite programming (SDP) relaxation is utilized to convert the original non-convex nonlinear model into an SDP model which can be solved efficiently by commercial solvers. Two case studies demonstrations are conducted on IEEE 13-node and 123-node three-phase networks. It is found that multi-terminal PC-SOPs can minimize power losses by between 5.56 % and 28.98% and have better voltage control (all buses operate in the allowed voltage range [0.94, 1.10]) and less PV curtailment (reduced by at least 6.31 MW/24 h and 0.63 MW/24 h for the two test networks separately) when compared to conventional SOP technologies.

1. Introduction

Low-voltage power distribution networks commonly experience three-phase imbalance [1]. In modern active distribution networks (ADNs), various single-phase distributed energy resources (DERs) are being stochastically integrated, such as intermittent renewable distributed generation (DG), random charging/discharging of plug-in electric vehicles (PEVs) [2,3] and energy storage systems (ESSs). They bring not only integration benefits but also challenges that make the phase imbalance more complex. Unbalanced resource/load components can be identified and swapped (when applicable) across phases as a direct way of mitigation [4]. There have been many techniques and measures to mitigate the three-phase imbalance of the distribution network. From an optimizing operations aspect, these include hierarchical power oscillations optimization [5], Bacterial Foraging with Spiral Dynamic (BF-SD) for re-phasing simultaneously optimization, stochastic optimization for DG sizing and rephasing strategy [6] and reconfiguration with tie switches [7]. However, network reconfiguration with tie switches is with a response time typically between 1 and 100 s [8]. Conversely, conventional two-terminal soft open points (SOPs) [9], which are designed and installed to replace traditional tie switches with much shorter response time (20 ms), are proven to reduce power losses and simultaneously mitigate the three-phase imbalance [10]. Meanwhile, the short response time make SOPs have better adaptability to DG uncertainties than traditional tie switches, considering the system attains a steady state after DG synchronization within 0.2 s which is much shorter than network reconfiguration time 1 s to 100 s [11].

1.1. Literature about conventional SOP and OPF modeling

There are four basic topologies of SOPs: back-to-back voltage-source converters (B2B VSCs), multi-terminal voltage-source converters (multi-terminal VSCs), unified power flow controller (UPFC), and static synchronous series compensator (SSSC). The SOPs based on multi-terminal VSCs tend to provide the offer the greater flexibility to the network than other three topologies of SOPs when considering a

☆ The work is supported by the Engineering and Physical Sciences Research Council (EPSRC, United Kingdom) in project "Street2Grid — an electricity blockchain platform for P2P energy trading" (Reference: EP/S001778/2).

* Corresponding author.
E-mail address: Jin.Yang@glasgow.ac.uk (J. Yang).

https://doi.org/10.1016/j.ijepes.2022.108228
Received 23 October 2021; Received in revised form 18 March 2022; Accepted 9 April 2022
Available online 10 May 2022

Nomenclature

Parameters

γ^{VSC}	Loss index of voltage-source converters (VSCs)
$\overline{v_i}$	Upper limit for second-order decision variable of voltage at node i
$\underline{v_i}$	Lower limit for second-order decision variable of voltage at node i
S^{VSCx}	Capacity of VSCx
y_i	Nodal shunt capacitance of node i
z_{ij}	Branch resistance from node i to node j

Variables

$d^+_{i,t}$	Positive penalty variable at node i at time t
$d^-_{i,t}$	Negative penalty variable at node i at time t
$I_{ij,t}$	Branch current vector from node i to node j at time t
$l_{ij,t}$	Second-order decision variable of current from node i to node j at time t
$P_t^{VSCx,\varphi,loss}$	Active power loss of VSCx at phase φ at time t
$P_t^{VSCx,\varphi}$	Active power of VSCx at phase φ at time t
$Q_t^{VSCx,\varphi}$	Reactive power of VSCx at phase φ at time t
s_i	Nodal injection at node i, i.e. either loads or the net injection of a distributed energy resource
$S_{ij,t}$	Second-order decision variable of power from node i to node j at time t
V_0^{ref}	Nodal voltage vector at the source node
v_0^{ref}	Second-order decision variable at the source node
$V_{i,t}$	Nodal voltage vector at node i at time t
$v_{i,t}$	Second-order decision variable of voltage at node i at time t

Indices and sets

Ω_b	Set of all network branches
Ω_n	Set of all network nodes
φ	Phase A, B or C (a, b, or c)
H	Hermitian transpose
M	Penalty index
T	Set of time
$VSCx$	VSC1, VSC2 or VSC3
012	Symmetrical components
abc	Phase components

uniform deployment across all networks [12]. In Ref. [13], a multi-objective optimization approach is adopted for hosting capacity (HC) maximization via sequential network reconfiguration followed SOP placement. Ref. [14] proposes a holistic framework for determining the appropriate system configurations, sizes, and placement of DG units, as well as the sizes and allocation of SOPs, using a modified particle swarm optimization (PSO) algorithm. A new Analytical Target Cascading based (ATC-based) approach is developed for optimal scheduling of a Multi-Area Active Distribution Network (MA-ADN) with inter-area SOPs in Ref. [15]. A novel two-stage coordinated optimization method is developed for the network with energy storage integrated soft open points (E-SOPs) and a battery energy storage system (BESS) to solve uncertainties of distributed generations and loads in Ref. [16].

In research related to SOPs, convex optimization is widely used. Especially second-order-cone programming (SOCP) and semidefinite programming (SDP). There are three main reasons for this. First, the constraint of SOP, based on the B2B VSCs topology or multi-terminal VSCs topology, is a circle which is convex [12,17]. Second, although optimal power flow (OPF) problems, including single-phase OPF and three-phase OPF, are nonconvex, it has been proved that OPF problems can be converted into convex problems [18]. The exactness of converted models has been proved in [19]. Third, the intersection of any finite number of convex sets is a convex set [20]. Therefore, most of the planning and service scheduling restoration optimization problems of ADNs with SOPs can be converted into convex ADN power flow problems with convex SOP constraints.

Specifically, the SOCP models are used in most research to simulate single-phase networks with conventional two-terminal and multi-terminal SOPs which are compared and shown in Table 1. Advancing these, our SOP research work has identified three research focuses summarized below:

- How multi-terminal SOPs are used in three-phase networks.
- How to operate phase-changed SOPs (PC-SOPs).
- How to improve modeling accuracy for three-phase networks with SOPs.

1.2. Literature about convex optimization of ADN power flows

DC approximations (DC OPF algorithms) are normally used for transmission systems rather than distribution systems to instruct economic dispatch, considering power flows with asset thermal constraints. However, DC OPF cannot be used for quantifying losses, voltage constraints or reactive power flows in most situations which are required for distribution system optimization [21].

Jabr et al. [22] formulate the single-phase OPF in power distribution networks as a mixed-integer second order cone programming (MISOCP), for which the global optimal solution up to the desired accuracy can be found by using available commercial solvers. The solutions proposed are proved not singular by the convergence of the Newton–Raphson solving scheme.

The nonconvexity of the single-phase OPF problem is much weaker than that of the three-phase OPF problem [23]. In Ref. [24], the authors present a methodology for unbalanced three-phase OPF based on a quasi-Newton method (iterative method) and OpenDSS (electric power distribution systems simulator) [25] for Smart Grid distribution management system. In Ref. [26], the authors applied a bus-injection SDP to demonstrate the ability to attain the global optimal solution of the original non-convex OPF problem.

In Ref. [30], a proposed model is enhanced by applying the chordal extension of a partial matrix which reduces the number of variables, speeding up the solving process. They found that the branch-flow model SDP (BFM-SDP) avoids ill-conditioned operations to enhance the numerical stability of the bus-injection model semidefinite programming (BIM-SDP) when keeping the equivalence in the physical model. Wang, Zeyu et al. [31] use symmetrical components to reduce the coupling between the phases in the backbones of the distribution network to create a new SDP model which is more numerically stable and more accurate than the existing BFM-SDP model.

1.3. Summary and contributions

In this paper, an optimized operational strategy for unbalanced ADNs based on SOPs is proposed. It enhances the operation efficiency and reduces the three-phase imbalance. Different SOPs' installation strategies focusing on the optimization modeling are investigated. The contributions of this study can be summarized as follows:

Table 1
Comparison of existing research.

Ref.	Model	Phase	SOP type	Other resources	Objectives
[10]	BFM-SDP	Three	Two-terminal SOP	DGs	Minimize total power losses, voltage & current unbalanced conditions
[27]	MISOCP	Single	Two-terminal SOP	ESS, DG inverters and on load tap changers	Determine the locations and energy/ power capacities of distributed ESS
[17]	Enhanced SOCP with tighten relaxation	Single	Multi-terminal SOP	DGs	Mitigate the feeder load imbalance and reduce power losses
[28]	SOCP	Single	Two-terminal SOP, multi-terminal SOP and two-terminal SOP with ESS	DGs	Improve the DG penetration
[29]	Robust SOCP	Single	Two-terminal SOP	DGs with uncertainty	Address the uncertainties of photovoltaics (PVs)

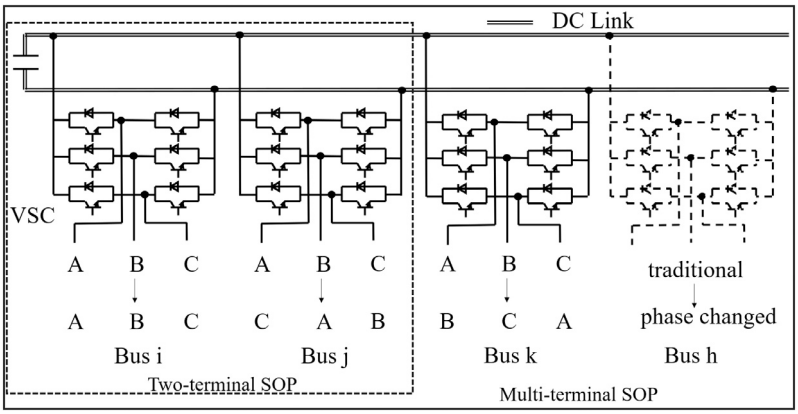

Fig. 1. Illustration and comparison of different SOPs.

- The potential of SOPs is explored by a new way of connection, i.e. power transferring between phases, so-called phase-changing SOP (PC-SOP). Compared with state-of-the-art approaches, the multi-terminal PC-SOPs for unbalanced three-phase networks are first proposed with unique advantages discussed. A multi-terminal PC-SOP based optimal operational strategy for unbalanced ADNs is proposed considering power losses and voltage deviation as a penalty.
- The OPF of three-phase unbalanced networks with SOPs is mathematically a non-convex nonlinear problem. Therefore, the symmetrical SDP formulation is used for the transformation of the original non-convex nonlinear model, for the OPF problem of three-phase unbalanced networks with SOPs. This approach can ensure the global optimum is obtained with an improved computational efficiency.
- Two case studies are conducted to optimize the regulations of SOPs and PV curtailment. Compared with other alternative SOP solutions, multi-terminal PC-SOP can reduce power losses by between 5.56% and 28.98%. This is a significant improvement simultaneously achieving effective voltage regulation.

The paper is organized as follows: Section 2 details the unbalanced optimal operation problem formulation. Section 3 details the converting to a symmetrical SDP model process. Section 4 presents the case studies with five different scenarios for comparison with result analysis. Section 5 summarizes the findings and concludes the paper.

2. Unbalanced optimal operation problem formulation

SOPs are power-electronic devices that are used to replace tie switches for network reconfiguration and offer further capabilities of accurate and flexible power flow control [32]. SOPs can transfer active power, supply reactive power and achieve real-time control of voltage between the connected feeders. Thereby cable power losses and risks caused by frequent switching actions in ADNs can be reduced.

2.1. Definition and configuration of different SOPs

2.1.1. Definition and configuration of two-terminal and multi-terminal conventional SOPs

B2B VSCs are the most commonly used SOP devices. Therefore normally they are used to analyze the optimization model for both the two-terminal [27,33] and multi-terminal SOPs [17] in steady-state operations. B2B VSCs can control three-phase active power and reactive power outputs independently [10]. One VSC of them operates in $V_{dc}f$ control mode; the other VSC(s) operate in PQ control mode. The loss index of each VSC can be 0.002 [17]. In a balanced system, three-phase feeders would be connected as balanced, i.e. corresponding phases (ABC to ABC) or (ABC to ABC to ABC) as shown in Fig. 1.

2.1.2. Definition and configuration two- and multi-terminal PC-SOPs

As the local DG outputs and electricity demand have inherent randomness, there is always a mismatch between them. Considering the B2B VSC implementation principle of employing a DC link to connect AC feeders, energy is transferred from AC to DC and then back to AC. As a result of connecting with PC-SOP, different phases of different feeders can be connected, which is advantageous in flexible operations of unbalanced systems. When DG outputs and electricity demand are distributed unevenly in different feeder phases, the whole network can achieve improved operating performances when phases can be indirectly connected by two-terminal PC-SOPs [34] marked by the dotted rectangle in Fig. 1. Therefore, compared with the traditional SOP structure, PC-SOPs can handle the mismatch caused by the intrinsic unpredictability of DG outputs and electricity demand.

In practical applications, insulated gate bipolar transistor (IGBT)-based VSCs with pulse width modulation can achieve the desired phase-changing function. Because IGBT-based VSCs are linked in parallel via a common DC link capacitor, complete control over the active power flowing across within its capacity limits, as well as independent

reactive power supply or absorption at both feeder terminals can be achieved [35].

New ways of connection of multi-terminal SOPs, called multi-terminal PC-SOPs (ABC to CAB to BCA, as a three-terminal example). In a multi-terminal PC-SOP, three-phase wires can be connected together between at least three buses, which means energy can be transferred amongst three phases of at least three feeders/buses marked by the solid line rectangle in Fig. 1. Operational constraints are expressed mathematically below.

Two-terminal PC-SOP operational constraints (e.g. ABC to CAB two-terminal PC-SOP):

$$\begin{cases} P_t^{VSC1,a} + P_t^{VSC2,c} + P_t^{VSC1,a,loss} + P_t^{VSC2,c,loss} = 0 \\ P_t^{VSC1,b} + P_t^{VSC2,a} + P_t^{VSC1,b,loss} + P_t^{VSC2,a,loss} = 0 \\ P_t^{VSC1,c} + P_t^{VSC2,b} + P_t^{VSC1,c,loss} + P_t^{VSC2,b,loss} = 0 \end{cases} \tag{1}$$

Multi-terminal PC-SOP operational constraints (e.g. ABC to CAB to BCA three-terminal PC-SOP):

$$\begin{cases} P_t^{VSC1,a} + P_t^{VSC2,c} + P_t^{VSC3,b} + P_t^{VSC1,a,loss} \\ +P_t^{VSC2,c,loss} + P_t^{VSC3,b,loss} = 0 \\ P_t^{VSC1,b} + P_t^{VSC2,a} + P_t^{VSC3,c} + P_t^{VSC1,b,loss} \\ +P_t^{VSC2,a,loss} + P_t^{VSC3,c,loss} = 0 \\ P_t^{VSC1,c} + P_t^{VSC2,b} + P_t^{VSC3,a} + P_t^{VSC1,c,loss} \\ +P_t^{VSC2,b,loss} + P_t^{VSC3,a,loss} = 0 \end{cases} \tag{2}$$

PC-SOP capacity and loss constraints:

$$\sqrt{P_t^{VSCx,\varphi^2} + Q_t^{VSCx,\varphi^2}} \le S^{VSCx^2} \tag{3}$$

$$P_t^{VSCx,\varphi,loss} = \gamma^{VSC}\sqrt{P_t^{VSCx,\varphi^2} + Q_t^{VSCx,\varphi^2}} \tag{4}$$

The PC-SOP capacity and loss constraints can be transferred into an SDP model for optimization ($\succeq$ means 'at least as good as' in SDP models [20]):

$$\begin{bmatrix} S^{VSCx} & P_t^{VSCx,\varphi} + jQ_t^{VSCx,\varphi} \\ P_t^{VSCx,\varphi} - jQ_t^{VSCx,\varphi} & S^{VSCx} \end{bmatrix} \succeq 0 \tag{5}$$

$$\begin{bmatrix} P_t^{VSCx,\varphi,loss}\gamma^{VSC} & P_t^{VSCx,\varphi} + jQ_t^{VSCx,\varphi} \\ P_t^{VSCx,\varphi} - jQ_t^{VSCx,\varphi} & P_t^{VSCx,\varphi,loss}/\gamma^{VSC} \end{bmatrix} \succeq 0 \tag{6}$$

2.2. Optimization modeling of three-phase ADNs with PVs, SOPs and voltage regulators

2.2.1. Objective function

This work aims to minimize an objective function comprising total power losses and voltage deviation penalties.

$$min\ f = f^{loss} + M \times \sum_{t=1}^{T}\sum_{i=1}^{\Omega_n}(d_{i,t}^{+} + d_{i,t}^{-}) \tag{7}$$

$$f^{loss} = \sum_{t=1}^{T}\Big(\sum_{ij\in\Omega_b} diag(l_{ij,t}z_{ij}) + \sum_{\substack{x=1,2,3 \\ \varphi=a,b,c}} P_t^{VSCx,\varphi,loss}\Big) \tag{8}$$

2.2.2. Three-phase system operational constraints

Power flow balance constraint at time t:

$$\sum_{ij\in\Omega_b} diag(S_{ij,t} - z_{ij}l_{ij,t}) + s_{j,t} + y_{j,t}v_{j,t} = \sum_{jk\in\Omega_b} diag(S_{jk,t}) \tag{9}$$

Kirchhoff's voltage constraints along line ij at time t:

$$v_{j,t} = v_{i,t} - (S_{ij,t}z_{ij}^H + S_{ij,t}^H z_{ij}) + z_{ij}l_{ij,t}z_{ij}^H \quad i \to j \tag{10}$$

$$\underline{v_i} \le diag(v_{i,t}) \le \overline{v_i} \tag{11}$$

$$v_0 = V_0^{ref}(V_0^{ref})^H \tag{12}$$

Eq. (13) expresses the positive semidefinite constraint where positive semidefinite matrix should have rank one, as enforces in (14).

$$\begin{bmatrix} v_{i,t} & S_{ij,t} \\ S_{ij,t}^H & l_{ij,t} \end{bmatrix} \succeq 0 \quad i \to j \tag{13}$$

$$rank\begin{bmatrix} v_{i,t} & S_{ij,t} \\ S_{ij,t}^H & l_{ij,t} \end{bmatrix} = 1 \quad i \to j \tag{14}$$

Node voltage, branch current and related second-order decision variables are defined as:

$$\begin{cases} V_{i,t} = \begin{bmatrix} V_{i,t}^a & V_{i,t}^b & V_{i,t}^c \end{bmatrix} \\ v_{i,t} = V_{i,t}V_{i,t}^H \\ I_{ij,t} = \begin{bmatrix} I_{ij,t}^a & I_{ij,t}^b & I_{ij,t}^c \end{bmatrix} \\ l_{ij,t} = I_{ij,t}I_{ij,t}^H \\ Sij = V_{i,t}I_{ij,t}^H \end{cases} \tag{15}$$

2.2.3. Modeling of voltage regulators

Ratios between the primary and secondary voltages are expressed as (Tap^{φ} is integer between [−16, 16].):

$$\begin{aligned} &ratio = \begin{bmatrix} r_t^a & r_t^b & r_t^c \end{bmatrix} \\ &V_{sec,t}^T = \begin{bmatrix} V_{sec,t}^a & V_{sec,t}^b & V_{sec,t}^c \end{bmatrix}^T = \begin{bmatrix} r_t^a V_{pri}^a & r_t^b V_{pri}^b & r_t^c V_{pri}^c \end{bmatrix} \\ &r_t^{\varphi} = 1 + 0.00625 \times Tap^{\varphi} \qquad \exists\ \varphi = a, b, c \end{aligned} \tag{16}$$

The voltages on the two sides of a regulator are linked as follows:

$$v_{sec,t}^{abc} = (v_{i,t} - (S_{reg,t}z_{reg}^H + S_{reg,t}^H z_{reg}) + z_{reg}l_{reg}z_{reg}^H) \cdot ratio \tag{17}$$

Converted into symmetrical components, (27) becomes:

$$Av_{sec,t}^{012}A^H = A[(v_{i,t}^{012} - (S_{reg,t}^{012}z_{reg}^{012,H} + S_{reg,t}^{012,H}z_{reg}^{012}) + z_{reg}^{012}l_{reg,t}^{012}z_{reg}^{012,H})]A^H \cdot ratio \tag{18}$$

where $V_{pri,t}^{\varphi}$ and $V_{sec,t}^{\varphi}$ are voltages of the regulator's primary side and secondary side at time t. $v_{sec,t}$ is the second-order decision variable of $V_{sec,t}$. $S_{reg,t}$ is the second-order decision variable of power for regulators at time t. z_{reg} is the regulator's resistance. $l_{reg,t}$ is the regulator's branch current vector.

2.2.4. Modeling of loads

Different models of loads are considered in this paper including constant impedance, constant current and constant power characteristics, also known as ZIP models [31].

Following the input of data such as network parameters, load profiles and SOP locations and sizes, the SDP problem is relaxed for SOP and power flow constraints. Then the optimization can be solved as an SDP OPF problem with power flows and variables considered for a 24-h simulation period, solved by MOSEK (commercial SDP solver) [36]. If all output voltages are within 0.2% deviation after multiple iterations, the solution achieves convergence and can be the final output. Otherwise the OPF results are used to update data until convergence is achieved.

3. Methodology: Converting to a symmetrical SDP model

The symmetrical components transformation reduces the phase coupling in three-phase systems [37]. Voltages in phase components are transformed into symmetrical components as follows:

$$V_{i,t}^{abc} = AV_{i,t}^{012} \tag{19}$$

Table 2
Optimization result comparison of the IEEE 13-node test feeder network.

	Case 0	Case 1	Case 2	Case 3	Case 4
Objective	189 470.00	17.51	15.45	16.09	13.30
Network losses (MW/24 h)	1488.80	16.01	13.70	14.52	11.37
Penalty function value	187 980.00	0.01	0.01	0.02	0.01
SOP losses (MW/24 h)	–	1.49	1.75	1.55	1.92
SOP transmit active power (MW/24 h)	–	7.90	17.36	8.81	21.34
SOP supply reactive power (MVAr/24 h)	–	69.31	70.32	74.21	75.36
PV active power (MW/24 h)	54.15	22.94	29.23	23.54	35.54
PV reactive power (MVAr/24 h)	15.63	6.01	7.16	6.20	6.67
Network imbalance index	19.58	15.82	15.08	15.92	14.80
Voltage deviation	10%/ −45.16%	6.14%/ −6.00%	6.40%/ −6.00%	10.00%/ −6.00%	10.00%/ −6.00%

$$A=\begin{bmatrix}1 & 1 & 1\\ 1 & a^2 & a\\ 1 & a & a^2\end{bmatrix} A^H = A^{-1} \tag{20}$$

where $a = 1\angle 120°$. Hence, the three-phase variables in the BFM-SDP method and the impedance parameters are related to the equivalent variables in symmetrical components:

$$\begin{cases} v_{i,t}^{abc} = V_{i,t}^{abc} \times V_{i,t}^{abc,H} = AV_{i,t}^{012} \times (AV_{i,t}^{012})^H = AV^{012}A^H \\ I_{i,t}^{abc} = AI_{i,t}^{012}A^H \\ S_{i,t}^{abc} = AS_{i,t}^{012}A^H \\ z_{i,t}^{abc} = Az_{i,t}^{012}A^{-1} = Az_{i,t}^{012}A^H \\ y_{i,t}^{abc} = Ay_{i,t}^{012}A^{-1} = Ay_{i,t}^{012}A^H \end{cases} \tag{21}$$

Objective function (8) and constraints (9)–(13) are transformed as follows (22)–(28). Penalty factors are introduced in voltage constraints (28):

$$f^{loss} = \sum_{t=1}^{T}\Big(\sum_{ij\in\Omega_b} diag(A(I_{ij,t}^{012}z_{ij}^{012})A^H) + \sum_{\substack{x=1,2,3\\ \varphi=a,b,c}} P_{\varphi,t}^{VSCx,loss}\Big) \tag{22}$$

$$\sum_{ij\in\Omega_b} diag(A(S_{ij,t}^{012} - z_{ij}^{012}I_{ij,t}^{012})A^H) + s_{j,t} + y_{j,t}^{012}v_{j,t}^{012} = \sum_{jk\in\Omega_b} diag(AS_{jk,t}^{012}A^H) \tag{23}$$

$$v_{j,t}^{012} = v_{i,t}^{012} - (S_{ij,t}^{012}z_{ij}^{012,H} + S_{ij,t}^{012,H}z_{ij}) + z_{ij}I_{ij,t}^{012}z_{ij}^{012,H} \tag{24}$$

$$\underline{v_{i,t}} \le diag(Av_{i,t}^{012}A^H) \le \overline{v_{i,t}} \tag{25}$$

$$v_0^{012} = V_0^{012,ref}(V_0^{012,ref})^H \tag{26}$$

$$\begin{bmatrix} v_i^{012} & S_{ij}^{012} \\ S_{ij}^{012,H} & I_{ij}^{012}\end{bmatrix} \succeq 0 \; i \to j \tag{27}$$

$$\begin{aligned} &diag(Av_{i,t}^{012}A^H) + d_{i,t}^{+} \ge \underline{v_{i,t}},\\ &diag(Av_{i,t}^{012}A^H) - d_{i,t}^{-} \le \overline{v_{i,t}},\\ &d_{i,t}^{+}, d_{i,t}^{-} \ge 0 \end{aligned} \tag{28}$$

4. Case studies, simulation results and discussion

The symmetrical SDP approach proposed in this paper is coded with YALMIP [38], and solved by MOSEK. The operating environment is Intel i7-10850H 2.7 GHz CPU, 32 GB RAM. Penalty index M in the penalty function is set to 1000.

4.1. Case study of IEEE 13-node test feeder with three-terminal PC-SOP

In this section, the IEEE 13-node test feeder [39], as shown in Fig. 2, is used as the test network to implement and validate the proposed model. The total capacity of the SOP is 2 MVA. SOPs are normally connected with end terminal buses. The SOP is located between buses 634, 675 and 680 which are three-phase. Conversely, lines 645–646, 684–652 and 684–611 are two-phase, single-phase and single-phase separately which cannot connect three-phase SOP. For the original IEEE 13-node test feeder, there is an imbalance problem caused by single-phase loads (1158 kW + 606 kVAr in Phase A, 973 kW + 672 kVAr in phase B, and 1135 kW + 753 kVAr in phase C, 3.827 times of standard total load at peaking time, shown in Fig. 2). Single-phase PV installations worsen this situation. 2 MVA capacity is used not only for the imbalance caused by the 10 MVA PV but also the maximum 904.28 kVA (707.99 kW & 562.56 kVAr) imbalance in the system. This test feeder illustrates particularly on advantages of the Phase-Changing technique in avoiding PV curtailment. Therefore, enough SOP capacity can promise clear demonstration results. It can be two 1 MVA two-terminal SOPs (SOP1 and SOP2) or one 2 MVA three-terminal SOP (SOP3). There are two 5 MVA PV installations located at buses 634 (phase B) and 646 (phases B and C). The power factor of PV generation is 0.95. The voltage range of all buses is set to be $[0.94, 1.10]$ as the statutory limits in the UK [40]. The three-phase regulator between buses 650 and 632 is set as $[r_t^a \; r_t^b \; r_t^c] = [1.05 \; 1.0375 \; 1.04375]$, same parameters as the example case in OpenDss.

Five cases are designed to demonstrate the benefits of multi-terminal PC-SOPs. PC-SOP connection ways (including Case 2 and 4) are shown in the table of Fig. 2. For Case 2, the connection way of SOP 1 is ABC to CAB and the connection way of SOP 2 is ABC to BCA. Therefore three phases are connected by two PC-SOPs. For Case 4, one three-terminal PC-SOP connects three-phase buses (ABC to CAB to BCA). It has been proved that the absolute deviations between the optimal selection of individual PC-SOP phase connections can be negligible [34].

Case 0: the original network
Case 1: the network with two two-terminal conventional SOPs.
Case 2: the network with two two-terminal PC-SOPs.
Case 3: the network with one three-terminal conventional SOP.
Case 4: the network with one three-terminal PC-SOP.

Network imbalance index for 24 h can be calculated as [10]:

$$\lambda_{UI,sys} = \sum_{t=1}^{T}\sum_{i=1}^{\Omega_n}\left(\frac{|V_{i,t}^A + aV_{i,t}^B + a^2V_{i,t}^C|}{|V_{i,t}^A + a^2V_{i,t}^B + aV_{i,t}^C|}\right) \tag{29}$$

4.2. Simulation result and discussion of IEEE 13-node test feeder with three-terminal PC-SOP

The results in Table 2 show that the three-terminal PC-SOP achieves the best objective value (13.30) with minimum network losses, the lowest network imbalance index (11.37 MW/24 h and 14.80 respectively). Without SOP, the original network voltages drop out of the low bound (−45.16%). Therefore the penalty function value is the

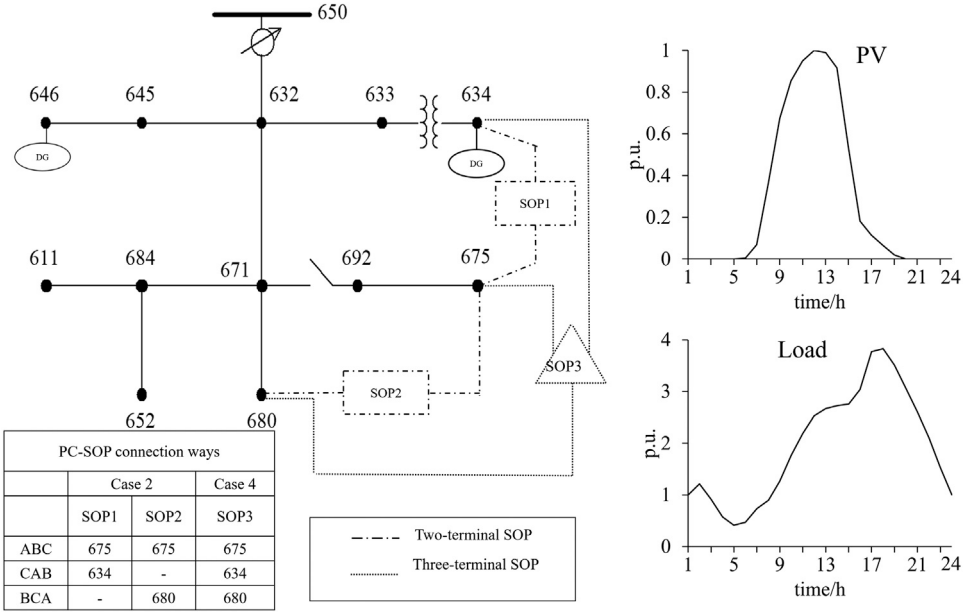

PC-SOP connection ways			
	Case 2		Case 4
	SOP1	SOP2	SOP3
ABC	675	675	675
CAB	634	-	634
BCA	-	680	680

Fig. 2. Test network with IEEE 13-node topology and profiles.

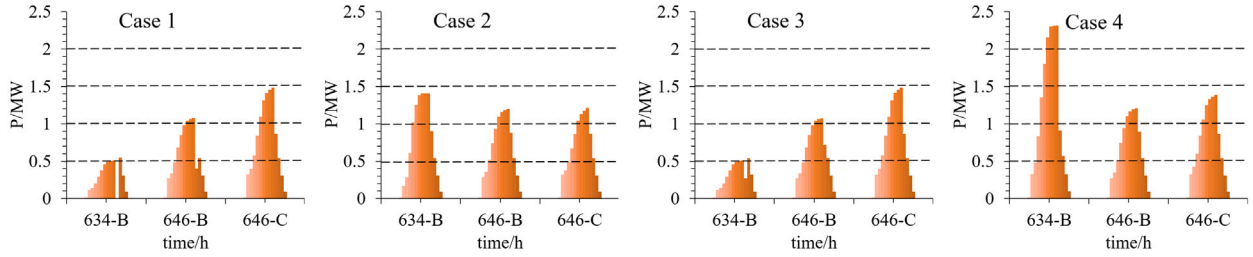

Fig. 3. Actual PV outputs.

highest (189470.00). That causes the highest network losses (1488.80 MW/24 h), the highest network imbalance index (19.58). All SOP solutions improve the original networks performance. The objective value shows phase-changing solution (Case 2, 15.45) and multi-terminal solution (Case 3, 16.09) achieve better performance than two-terminal conventional SOPs in Case 1. Both Case 2 (17.36 MW/24 h) and Case 3 (8.81 MW/24 h) can transmit more active power than Case 1 (7.90 MW/24 h). Although PV output is the highest in Cases 0, it can be ignored because system cannot operate within that voltage range. Except Case 0, Case 2, 3, 4 can improve PV output compared with Case 1. Especially, PV active power in Case 4 (35.54 MW/24 h) is the highest among Cases 1–4. Therefore both phase changing and multi-terminal solutions for SOPs can achieve better objective values than the normal solution for SOP considering network losses. In addition, the combination solution (Case 4, which combines multi-terminal with phase-changing) can achieve better performance compared with individual solutions.

In Fig. 3, Case 4 shows maximized PV outputs for all installation locations; while Case 1 shows the overall minimal among Cases 1–4 . For two-phase PV 646, there is nearly the same PV curtailment in all four Cases. This is due to that PV 646 is on the opposite side of SOPs in the network. PV 634 hardly generates power which ranges from 0 to 0.6 kW in Cases 1 and 3. However, the PC-SOP in Case 2 and Case 4 can make the network effectively utilize different phase resources — the outputs of PV 634 in Case 2 exceed 1 MW and PV 634 in Case 4 exceed 2 MW, because the PC-SOP effectively acts as a 'bridge' to provide a path for power transfer between DG and loads from different phases (between PVs in phase B and the load demand in phases A and C). One multi-terminal PC-SOP can be more effective in phase connection than two separate two-terminal PC-SOPs with the same total capacity.Also, PC-SOP 'bridge' function enhances the adaptability to DG uncertainties between different phases for its better usage of power transfer capacity.

4.3. Case study of IEEE 123-node test feeder with four-terminal PC-SOP

In [10], a modified IEEE 123-node distribution network is used to verify the scalability of the optimal operation of multi-terminal on large-scale ADNs with severe unbalanced conditions. In [34], PC-SOP has been proved that it can transmit more active power and utilize its capacity better than conventional SOP. However, in the original network, the line segment between bus 93 and 94 is single-phase (A-N), and bus 94 is single-phase [39], as shown in Fig. 4. The tie switch between bus 54 and bus 94 is moved to between bus 54 and bus 93 to keep the original line configurations, because bus 93 is three-phase and SOP normally connects with three-phase buses.

Other DGs' parameters and total SOP's capacity are the same as the data in [10]. PV generation and load profiles are the same as shown in Fig. 2. The regulators are set as $[r_t^a\ r_t^b\ r_t^c] = [1.04375\ 1.04375\ 1.04375]$ (buses 150 to 149, three-phase regulator), $r_t^a = 0.99375$ (buses 9 to 14, single-phase regulator), $[r_t^a\ r_t^c] = [0\ 0.99375]$ (buses 25 to 26, two-phase regulator), $[r_t^a\ r_t^b\ r_t^c] = [1.5\ 1.00625\ 1.3125]$ (buses 67 to 160, two-phase regulator), same parameters as the example case in OpenDss. The load at bus 610 connected to the secondary is directly connect to the primary bus 61.

Similar to Section 4.1, five cases are designed to show the benefits of multi-terminal PC-SOPs. The difference with Section 4.1, is that in this section Cases 3 and 4 aim at proving the benefits of four-terminal SOPs. Meanwhile, an assumption is made that the physical distances

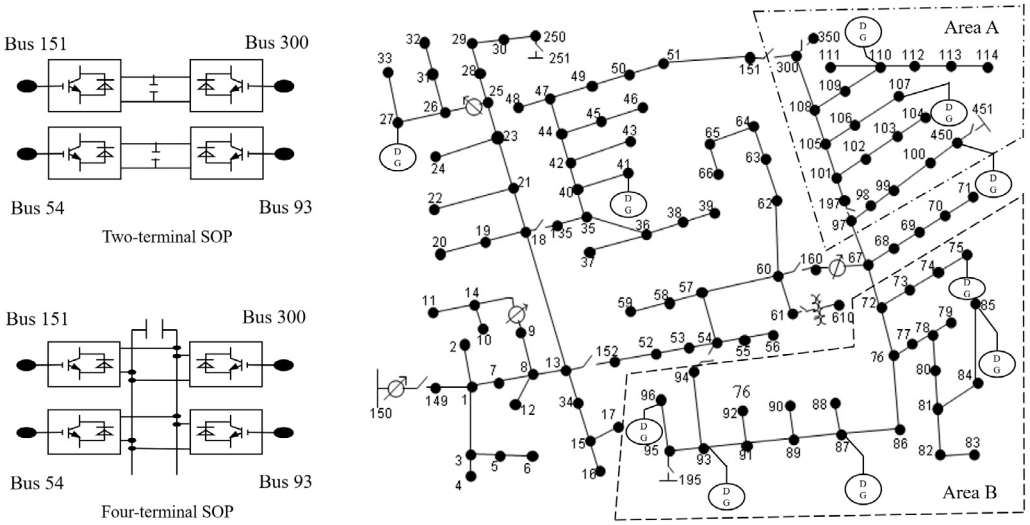

Fig. 4. Test network with IEEE 123-node topology.

Table 3
Optimization result comparison of the IEEE 123-Node test feeder network.

	Case 0	Case 1	Case 2	Case 3	Case 4
Objective	80 229.00	14.14	13.29	10.33	9.91
Network losses (MW/24 h)	66.85	12.90	11.96	8.85	8.34
Penalty function value	80 162.00	0.14	0.15	0.13	0.14
SOP losses (MW/24 h)	–	1.10	1.18	1.35	1.43
SOP transmit active power (MW/24 h)	–	12.45	14.08	19.56	21.84
SOP supply reactive power (MVAr/24 h)	–	47.08	48.61	52.30	52.83
PV active power (MW/24 h)	4.08	4.71	4.71	4.71	4.71
Network imbalance index	23.05	22.11	15.83	22.99	14.49
Voltage deviation	9.82%/ −13.14%	9.64%/ −6.00%	9.64%/ −6.00%	9.64%/ −6.00%	9.64%/ −6.00%

between buses 54, 93, 151 and 300 are not too far from each other to be connected with a multi-terminal SOP.

4.4. Simulation results and discussion of IEEE 123-node test feeder with four-terminal PC-SOP

The results in Table 3 show that the four-terminal PC-SOP achieves the best objective value (9.91) with minimum network losses, the lowest network imbalance index (8.34 MW/24 h and 14.49 respectively). Without SOP, the original network voltages drop below the low bound (−13.14%). Therefore the penalty function value is the highest (80162.00). That causes the highest network losses (66.85 MW/24 h), the highest network imbalance index (23.05). All SOP solutions improve the original networks performance. The objective value shows the phase-changed solution (Case 2, 13.29) and the multi-terminal solution (Case 3, 10.33) achieve better performance than two-terminal conventional SOPs in Case 1. However, compared with Section III-A, here the Case 3's objective value is better than the Case 2. Therefore, it proves that both multi-terminal and PC-SOP solutions can improve networks' performance. The multi-terminal solution has the advantage in improving load distribution imbalance in the whole network. While the PC-SOP solution has the advantage in balancing DG and load distributions in different phases.

The multi-terminal PC-SOP, compared with the conventional SOP, two-terminal PC-SOP and multi-terminal SOP, can transfer more power and utilize the network capacity better in unbalanced networks. As shown in Fig. 5, the differences in the transmitted power between different cases at hour 18 (peak load hour) are analyzed in detail as follows:

- In general, power is transferred from the network left side (bus 151 and bus 54) to the network right side (bus 300 and bus 93) because the substation is installed at the left (bus 150).
- The operational power of the multi-terminal PC-SOP is greater than those of the other 3 cases. The average active power of the multi-terminal PC-SOP is 423.55 kW. The average active powers of the other 3 cases are 137.08, 126.85 and 403.70 kW.
- In the Area A (from bus 97 to bus 450), Phase A load is the highest among three phases (Phase A: 688.92 kW, Phase B:459.28 kW, Phase C: 535.82 kW at hour 18) and in the Area B (bus 72 to bus 96), Phase C load is the highest among three phases (Phase A: 1014.24 kW, Phase B:1109.92 kW, Phase C: 1186.47 kW at hour 18). In Cases 2 to 4, SOP mainly transmit active power to Phase A at bus 300 and Phase C at bus 93. However, SOP cannot achieve this in Case 1. Meanwhile, the multi-terminal PC-SOP can transmit the highest power (562.27 kW and 644.83 kW). Therefore, Case 4 achieves the minimum objective value (1.39) at hour 18.

4.5. Algorithm validation of case studies

The computation information of the Case 4 is shown in Table 4 to demonstrate the superior numerical stability of the symmetrical SDP over the BFM-SDP. The results obtained with the BSM-SDP OPF and the symmetrical SDP OPF are compared with the OpenDSS benchmark results based on the absolute percentage errors of the voltages. The computation efficiency and robustness of the proposed method is demonstrated by comparing results with the Interior Point OPTimizer (IPOPT, a software library for large scale nonlinear optimization of continuous systems) [41].

$$Error_{v}^{\phi} = \left| \frac{v_{SDP}^{\phi} - v_{OpenDSS}^{\phi}}{v_{OpenDSS}^{\phi}} \right| \times 100\% \tag{30}$$

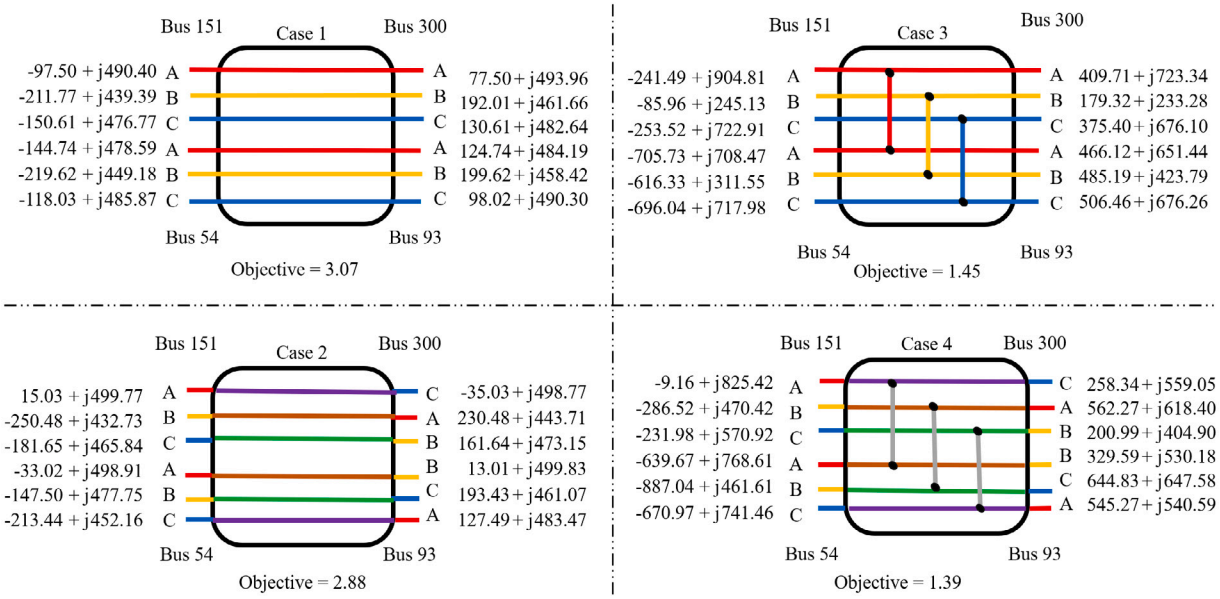

Fig. 5. SOP power flows outcome (kVA).

Table 4
OPF solution time and voltage error on various test feeders.

Test feeder	IEEE 13-node				IEEE 123-node			
	Voltage error%			Time (s)	Voltage error%			Time (s)
	Phase A	Phase B	Phase C		Phase A	Phase B	Phase C	
BFM-SDP (Sedumi)	2.103%	1.652%	1.451%	41.72	1.055%	2.422%	1.445%	202.23
BFM-SDP (Mosek)	–	–	–	–	–	–	–	–
Sym.SDP (Sedumi)	0.037%	0.028%	0.026%	39.59	0.014%	0.029%	0.018%	191.91
Sym.SDP (Mosek)	0.036%	0.028%	0.026%	12.53	0.014%	0.029%	0.018%	60.74
IPOPT	0.036%	0.028%	0.026%	116.09	0.014%	0.029%	0.018%	562.77

It is shown that the symmetrical SDP method achieves a voltage error of less than 0.2% which is smaller compared with the BFM-SDP. Based on [31], this paper further proves that symmetrical SDP is more accurate and efficient compared with BFM-SDP in networks with multi-terminal SOPs with the SeDuMi (open-source SDP solver) [42] and MOSEK. Owing to the proper relaxation of the original problem with convexification, the symmetrical SDP method reduces the solving complexity (12.53 s for IEEE 13-node test feeder and 60.74 s for IEEE 123-node test feeder — both for 24-h network operation) and obtains the solution within a reasonable accuracy. This creates possibilities for modeling larger test feeders (e.g. IEEE 8500-node test feeder). Nodal voltages for the IEEE 13-node test feeder at hour 1 as an example are shown in Table 5. When multi-terminal PC-SOP outputs are: Phase A $[0 + j0; 0 + j0; 0 + j0]$ kVA, Phase B $[44.356 + j78.027; -7.388 + j0.842; 13.632 + j244.930]$ kVA and Phase C $[-15.150 + j68.443; -50.163 + j46.362; 4.190 + j44.788]$ kVA, all voltage errors are within 2%.

Table 5
Nodal voltages for the IEEE 13-node test feeder.

Bus	Symmetrical SDP			OpenDSS		
	Phase A	Phase B	Phase C	Phase A	Phase B	Phase C
SOURCEBUS	1	1	1	1	1	1
650	0.9999	0.9999	0.9999	1	1	1
RG60	1.0499	1.0374	1.0437	1.0498	1.0374	1.0436
633	1.0131	1.02	1.0087	1.0127	1.0202	1.0084
634	0.9963	1.0035	0.9955	0.9959	1.0037	0.9952
671	0.9893	1.0248	0.9871	0.9885	1.0258	0.9876
645	0	1.0127	1.0087	0	1.0128	1.0084
646	0	1.0109	1.0066	0	1.0111	1.0064
692	0.9893	1.0248	0.9871	0.9885	1.0258	0.9876
675	0.9851	1.0261	0.9868	0.9842	1.0271	0.9873
611	0	0	0.9831	0	0	0.9836
652	0.9818	0	0	0.981	0	0
632	1.0156	1.0219	1.0106	1.0153	1.0221	1.0103
680	0.9893	1.0248	0.9871	0.9885	1.0258	0.9876
684	0.9874	0	0.9851	0.9866	0	0.9856

5. Conclusion

This paper compares different SOP configurations for multiple buses in power distribution networks. An optimized operational strategy based on various connection ways and a new multi-terminal PC-SOP connection is proposed to minimize the operational losses considering the growing penetration levels of DERs for unbalanced three-phase networks. The optimization results indicate that the multi-terminal and PC-SOP cases significantly reduce unbalanced loading conditions and power losses in ADNs. For distribution network operators, it can help to achieve a 24-h optimal ADN schedule with the addition of flexible and controllable resources such as conventional SOPs, PC-SOPs and PVs in smart ADNs.

One of the limitations of the current study is that transient operational performance has not been carried out with hardware design and simulations which are required for further implementation. Also, the control and coordination considering time-response between PC-SOPs and other phase transferring techniques require further research, taking into account the robustness of the three-phase unbalanced network optimization and capital investment and operational costs of these new power-electronic switches.

CRediT authorship contribution statement

Chengwei Lou: Conceptualization, Methodology, Programming, Writing – original draft. **Jin Yang:** Conceptualization, Methodology,

Supervision, Reviewing and editing. **Eduardo Vega-Fuentes:** Reviewing and editing. **Nand K. Meena:** Reviewing and editing. **Liang Min:** Reviewing, Result validation.

Declaration of competing interest

The authors declare that they have no known competing financial interests or personal relationships that could have appeared to influence the work reported in this paper.

Acknowledgments

Chengwei Lou would like to thank the China Scholarship Council (Reference: CSC201806350260) and the University of Glasgow for supporting his PhD study.

References

[1] Ma K, Li R, Li F. Utility-scale estimation of additional reinforcement cost from three-phase imbalance considering thermal constraints. IEEE Trans Power Syst 2017;32(5):3912–23.
[2] Xu T, Pan J, Jiang Y, Hou H, Li Y. The effect of three-phase voltage imbalance at PCC on solar panel output power. Procedia Comput Sci 2015;52:1218–24.
[3] Aramizu J, Vieira JC. Analysis of PV generation impacts on voltage imbalance and on voltage regulation in distribution networks. IEEE Power Energy Soc Gener Meet 2013;1–5. http://dx.doi.org/10.1109/PESMG.2013.6672822.
[4] Kong W, Ma K, Wu Q. Three-phase power imbalance decomposition into systematic imbalance and random imbalance. IEEE Trans Power Syst 2018;33(3):3001–12.
[5] Jin P, Li Y, Li G, Chen Z, Zhai X. Optimized hierarchical power oscillations control for distributed generation under unbalanced conditions. Appl Energy 2017;194:343–52.
[6] Soltani S, Rashidinejad M, Abdollahi A. Stochastic multiobjective distribution systems phase balancing considering distributed energy resources. IEEE Syst J 2017;12(3):2866–77.
[7] Borozan V, Rajicic D, Ackovski R. Minimum loss reconfiguration of unbalanced distribution networks. IEEE Trans Power Deliv 1997;12(1):435–42.
[8] ABB. Working with the trip characteristic curves of ABB SACE low voltage circuit-breakers. Technical application guide, 2001.
[9] Cao W, Wu J, Jenkins N. Feeder load balancing in MV distribution networks using soft normally-open points. In: IEEE PES innovative smart grid technologies conference Europe, Vol. 2015-January (January). 2015, p. 1–6. http://dx.doi.org/10.1109/ISGTEurope.2014.7028874.
[10] Li P, Ji H, Wang C, Zhao J, Song G, Ding F, Wu J. Optimal operation of soft open points in active distribution networks under three-phase unbalanced conditions. IEEE Trans Smart Grid 2019;10(1):380–91.
[11] Dewadasa M, Ghosh A, Ledwich G. Dynamic response of distributed generators in a hybrid microgrid. In: 2011 IEEE power and energy society general meeting. 2011, p. 1–8. http://dx.doi.org/10.1109/PES.2011.6039273.
[12] Bloemink JM, Green TC. Benefits of distribution-level power electronics for supporting distributed generation growth. IEEE Trans Power Deliv 2013;28(2):911–9.
[13] Ali ZM, Diaaeldin IM, El-Rafei A, Hasanien HM, Abdel Aleem SH, Abdelaziz AY. A novel distributed generation planning algorithm via graphically-based network reconfiguration and soft open points placement using archimedes optimization algorithm. Ain Shams Eng J 2021;12(2):1923–41. http://dx.doi.org/10.1016/j.asej.2020.12.006, URL https://www.sciencedirect.com/science/article/pii/S2090447921000186.
[14] Shafik MB, Chen H, Rashed GI, El-Sehiemy RA, Elkadeem MR, Wang S. Adequate topology for efficient energy resources utilization of active distribution networks equipped with soft open points. IEEE Access 2019;7:99003–16. http://dx.doi.org/10.1109/ACCESS.2019.2930631.
[15] Bastami H, Shakarami MR, Doostizadeh M. A decentralized cooperative framework for multi-area active distribution network in presence of inter-area soft open points. Appl Energy 2021;300:117416. http://dx.doi.org/10.1016/j.apenergy.2021.117416, URL https://www.sciencedirect.com/science/article/pii/S0306261921008126.
[16] Hu R, Wang W, Wu X, Chen Z, Ma W. Interval optimization based coordinated control for distribution networks with energy storage integrated soft open points. Int J Electr Power Energy Syst 2022;136:107725. http://dx.doi.org/10.1016/j.ijepes.2021.107725, URL https://www.sciencedirect.com/science/article/pii/S0142061521009510.
[17] Ji H, Wang C, Li P, Zhao J, Song G, Ding F, Wu J. An enhanced SOCP-based method for feeder load balancing using the multi-terminal soft open point in active distribution networks. Appl Energy 2017;208:986–95. http://dx.doi.org/10.1016/j.apenergy.2017.09.051.
[18] Low SH. Convex relaxation of optimal power flow—Part I: Formulations and equivalence. IEEE Trans Control Netw Syst 2014;1(1):15–27. http://dx.doi.org/10.1109/TCNS.2014.2309732.
[19] Low SH. Convex relaxation of optimal power flow—Part II: Exactness. IEEE Trans Control Netw Syst 2014;1(2):177–89. http://dx.doi.org/10.1109/TCNS.2014.2323634.
[20] Boyd S, Vandenberghe L. Convex optimization. Cambridge University Press; 2004.
[21] Coffrin C, Van Hentenryck P. A linear-programming approximation of AC power flows. INFORMS J Comput 2014;26(4):718–34. http://dx.doi.org/10.1287/ijoc.2014.0594, arXiv:arXiv:1206.3614v3.
[22] Jabr RA. Exploiting sparsity in SDP relaxations of the OPF problem. IEEE Trans Power Syst 2012;27(2):1138–9.
[23] Wang W, Yu N. Chordal conversion based convex iteration algorithm for three-phase optimal power flow problems. IEEE Trans Power Syst 2018;33(2):1603–13.
[24] Bruno S, Lamonaca S, Rotondo G, Stecchi U, La Scala M. Unbalanced three-phase optimal power flow for smart grids. IEEE Trans Ind Electron 2011;58(10):4504–13. http://dx.doi.org/10.1109/TIE.2011.2106099.
[25] Dugan RC, McDermott TE. An open source platform for collaborating on smart grid research. In: 2011 IEEE power and energy society general meeting. 2011, p. 1–7. http://dx.doi.org/10.1109/PES.2011.6039829.
[26] Dall'Anese E, Zhu H, Giannakis GB. Distributed optimal power flow for smart microgrids. IEEE Trans Smart Grid 2013;4(3):1464–75. http://dx.doi.org/10.1109/TSG.2013.2248175.
[27] Bai L, Jiang T, Li F, Chen H, Li X. Distributed energy storage planning in soft open point based active distribution networks incorporating network reconfiguration and DG reactive power capability. Appl Energy 2018;210:1082–91. http://dx.doi.org/10.1016/j.apenergy.2017.07.004.
[28] Ji H, Wang C, Li P, Zhao J, Song G, Wu J. Quantified flexibility evaluation of soft open points to improve distributed generator penetration in active distribution networks based on difference-of-convex programming. Appl Energy 2018;218:338–48. http://dx.doi.org/10.1016/j.apenergy.2018.02.170.
[29] Ji H, Wang C, Li P, Ding F, Wu J. Robust operation of soft open points in active distribution networks with high penetration of photovoltaic integration. IEEE Trans Sustain Energy 2019;10(1):280–9. http://dx.doi.org/10.1109/TSTE.2018.2833545.
[30] Gan L, Low SH. Convex relaxations and linear approximation for optimal power flow in multiphase radial networks. In: 2014 power systems computation conference. 2014, p. 1–9. http://dx.doi.org/10.1109/PSCC.2014.7038399.
[31] Wang Z, Kirschen DS, Zhang B. Accurate semidefinite programming models for optimal power flow in distribution systems. 2017, arXiv preprint arXiv:1711.07853.
[32] Long C, Wu J, Thomas L, Jenkins N. Optimal operation of soft open points in medium voltage electrical distribution networks with distributed generation. Appl Energy 2016;184:427–37. http://dx.doi.org/10.1016/j.apenergy.2016.10.031.
[33] Cao W, Wu J, Jenkins N, Wang C, Green T. Benefits analysis of soft open points for electrical distribution network operation. Appl Energy 2016;165:36–47. http://dx.doi.org/10.1016/j.apenergy.2015.12.022.
[34] Lou C, Yang J, Li T, Vega-Fuentes E. New phase-changing soft open point and impacts on optimising unbalanced power distribution networks. IET Gener Transm Distrib 2020;14(23):5685–96. http://dx.doi.org/10.1049/iet-gtd.2019.1660.
[35] Perales M, Prats M, Portillo R, Mora J, Leon J, Franquelo L. Three-dimensional space vector modulation in abc coordinates for four-leg voltage source converters. IEEE Power Electron Lett 2003;1(4):104–9. http://dx.doi.org/10.1109/LPEL.2004.825553.
[36] ApS M. The MOSEK optimization toolbox for MATLAB manual. Version 9.0. 2019, URL http://docs.mosek.com/9.0/toolbox/index.html.
[37] Lou C, Yang J, Min L. Symmetrical semidefinite programming with bifurcation phase-changing SOPs for unbalanced power distribution networks. In: 2021 IEEE 5th conference on energy internet and energy system integration (EI2). 2021, p. 1242–7. http://dx.doi.org/10.1109/EI252483.2021.9713647.
[38] Lofberg J. YALMIP: A toolbox for modeling and optimization in MATLAB. In: 2004 IEEE international conference on robotics and automation (IEEE cat. no. 04CH37508). IEEE; 2004, p. 284–9.
[39] Kersting WH. Radial distribution test feeders. IEEE Trans Power Syst 1991;6(3):975–85.
[40] Smith A. Electricity safety, quality and continuity regulations 2002. Light J 2003;68(2):35–6.
[41] Wächter A, Biegler LT. On the implementation of an interior-point filter line-search algorithm for large-scale nonlinear programming. Math Program 2006;106(1):25–57.
[42] Sturm JF. Using SeDuMi 1.02, a MATLAB toolbox for optimization over symmetric cones. Optim Methods Softw 1999;11(1–4):625–53.